

Quantum Machine Learning Predicting ADME-Tox Properties in Drug Discovery

Amandeep Singh Bhatia,* Mandeep Kaur Saggi,* and Sabre Kais*

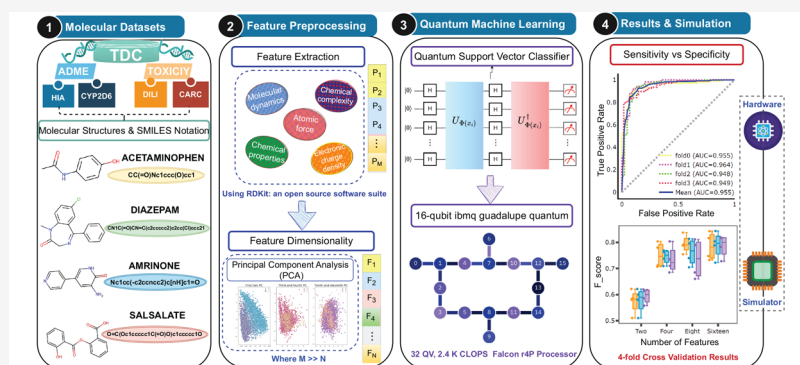
Cite This: <https://doi.org/10.1021/acs.jcim.3c01079>

Read Online

ACCESS |

Metrics & More

Article Recommendations



ABSTRACT: In the drug discovery paradigm, the evaluation of absorption, distribution, metabolism, and excretion (ADME) and toxicity properties of new chemical entities is one of the most critical issues, which is a time-consuming process, immensely expensive, and poses formidable challenges in pharmaceutical R&D. In recent years, emerging technologies like artificial intelligence (AI), big data, and cloud technologies have garnered great attention to predict the ADME and toxicity of molecules. Currently, the blend of quantum computation and machine learning has attracted considerable attention in almost every field ranging from chemistry to biomedicine and several engineering disciplines as well. Quantum computers have the potential to bring advances in high-throughput experimental techniques and in screening billions of molecules by reducing development costs and time associated with the drug discovery process. Motivated by the efficiency of quantum kernel methods, we proposed a quantum machine learning (QML) framework consisting of a classical support vector classifier algorithm with a kernel-based quantum classifier. To demonstrate the feasibility of the proposed QML framework, the simplified molecular input line entry system (SMILES) notation-based string kernel, combined with a quantum support vector classifier, is used for the evaluation of chemical/drug ADME-Tox properties. The proposed quantum machine learning framework is validated and assessed via large-scale simulations. Based on our results from numerical simulations, the quantum model achieved the best performance as compared to classical counterparts in terms of the area under the curve of the receiver operating characteristic curve (AUC ROC; 0.80–0.95) for predicting outcomes on ADME-Tox data sets for small molecules, with a different number of features. The deployment of the proposed framework in the pharmaceutical industry would be extremely valuable in making the best decisions possible.

1. INTRODUCTION

In drug development, accurately predicting the absorption, distribution, metabolism, and excretion (ADME) properties of chemical compounds is challenging due to complex physiological mechanisms. Characterization of ADME properties of a drug in the body is indeed an essential prerequisite for evaluating drug efficacy and safety.^{1,2} In fact, unfavorable ADME properties lead to 40% of drug failures overall, which is a significant factor contributing to the failure of candidate molecules.³ In the pharmaceutical industry, the early prediction of ADME properties has gained significant interest with an objective of improving the success rate of compounds reaching further in the discovery and development stages. Every year, a vast number of chemical compounds produced globally, combined with the

potential for toxicity, poses a significant task for researchers and toxicologists.⁴ Toxicology is the study that focuses on the adverse effects (i.e., death or injury) that chemical or physical agents can have on living organisms. Unfortunately, unfavorable ADME-Tox properties are one of the leading causes of drug withdrawals in the preclinical or clinical trials.⁵ To address these

Received: July 15, 2023

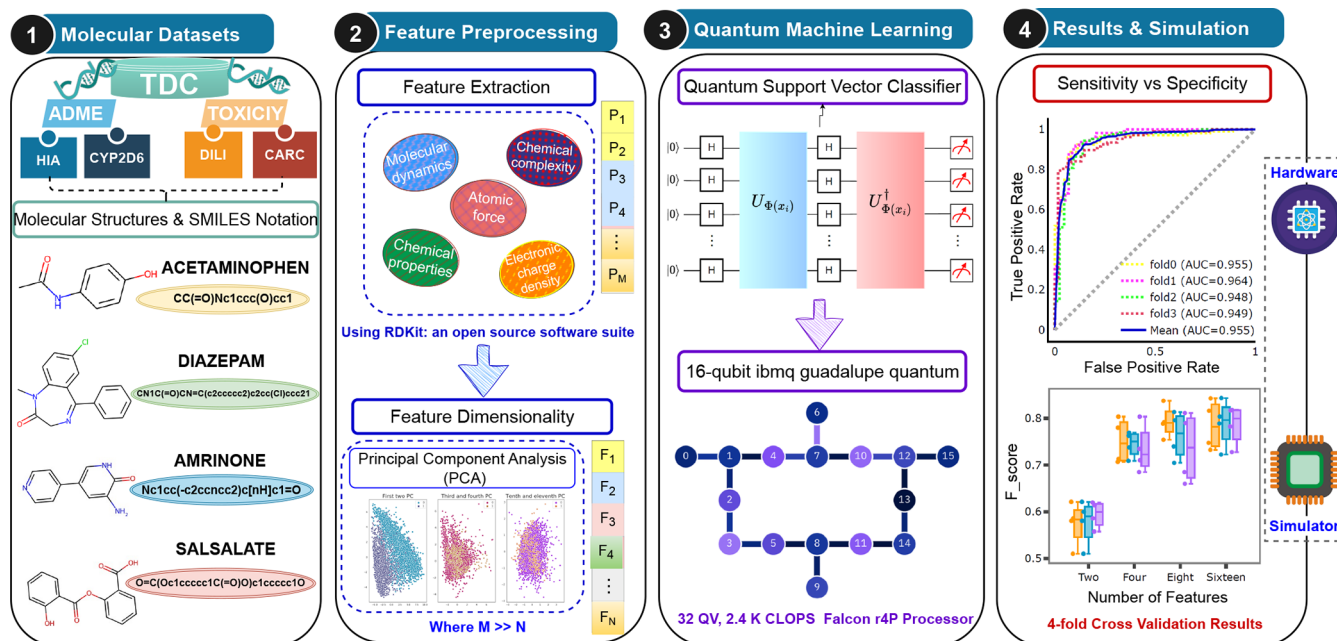


Figure 1. An overview of the quantum machine learning framework for predicting ADME and toxicity properties. (1) ADME-Tox data sets and their molecular structures and SMILES notations. (2) Feature processing and feature dimension reduction using PCA. (3) Quantum classifier for predicting ADME-Tox properties on quantum simulator and hardware. (d) Classification metrics.

challenges, advances in computational modeling techniques, improved data integration and sharing, and the development of alternative testing models can be of great help.^{6–8}

In recent years, the realm of quantum computing has held significant potential to solve complex computational problems more efficiently, which are beyond classical boundaries.⁹ Researchers and scientists are actively working toward unlocking the full potential of quantum computing and exploring its practical applications.¹⁰ Currently, the blend of quantum computing and machine learning is a rapidly evolving field, and there have been several notable advances in several domains ranging from healthcare to finance to chemistry.^{11–14}

The collaboration between academic institutions, research communities, and pharmaceutical industries has been making significant contributions to drug discovery by leveraging the power of quantum computing with machine learning techniques,¹⁵ such as quantum kernel methods (i.e., quantum support vector classifier (QSVC)),¹⁶ quantum generative models (i.e., quantum generative adversarial networks),^{17,18} matrix product-state-based quantum classifiers,²² quantum-enhanced optimization (i.e., quantum approximate optimization algorithm (QAOA), variational quantum eigensolver (VQE)¹⁹), and physicochemical applications.²⁰ It has been observed that quantum kernel methods can efficiently produce complex patterns in terms of quantum circuit training speed and accuracy of the classifier. However, the application of QML algorithms to the drug discovery pipeline is still in its early stages, and its practical applications are limited by the size and computational power of today's quantum computers.

While quantum computers with machine learning hold great promise, for drug discovery, there are several challenges and complications to predicting ADME-Tox properties such as training data availability (i.e., collecting ADME-Tox data sets with sufficient diversity can be difficult due to experimental constraints), quantum data representation (i.e., an effective method is required to represent the database of molecules into a

quantum format), and scaling and generalization (i.e., scaling of quantum algorithms to process larger data sets can become a significant challenge).

1.A. Motivation. The ADME-Tox properties depend on multiple factors and involve complex processes that often are interconnected. Typically, chemists predict these properties using diverse machine learning models, such as linear regression models, regression trees, neural networks, or support vector machines. Quantum machine learning has the potential to accelerate the drug discovery process, enable more efficient identification of novel drug candidates, and improve molecule design. Motivated by the exponential advantage of the quantum support vector classifier over classical algorithms and its robustness to noise, we proposed a quantum machine learning (QML) framework employing a QSVC to predict ADME-Tox properties of chemical compounds in drug discovery, as shown in Figure 1.

The quantum classifier (quantum support vector classifier (QSVC)²¹) using *n*-fold cross-validation is learning molecular properties from string-based chemical representations such as SMILES. To demonstrate the feasibility of the proposed QML framework, we performed extensive experiments on benchmarking data sets of ADME (i.e., HIA (human intestinal absorption),²⁴ CYP2D6 Substrate (dominantly expressed in the liver),²³ Tox properties (DILI (drug-induced liver injury)²⁶), and Carcinogens (promotes the formation of cancer).²⁵ Based on our results from numerical IBMQ simulations and IBMQ hardware, we demonstrate that the quantum classifier is capable of learning to identify important ADME-Tox properties and has a significantly enhanced performance. The proposed framework can be applied to any SMILES strings of chemical compounds against a desired target (i.e., active or inactive, classification of substrates and nonsubstrates). Moreover, the proposed framework can be demonstrated in federated settings for collaborative drug discovery across the pharmaceutical industry.²³

The remainder of this article is organized as follows: Section II is related work. Section III presents the problem formulation, methodology, and description of benchmarking chemical data sets used in the study. Moreover, the SVC and QSVC are described in section III.B. Section IV presents the experimental results from the IBM simulator with and without noise and a discussion of the findings and outcomes. Finally, the concluding remarks are reported in section V.

II. PRIOR WORK

Today's variational quantum algorithms (VQE or QAOA) are designed to be implemented on the current generation of quantum systems known as noisy intermediate-scale quantum (NISQ) devices.²⁹ Sen et al.²⁸ tackled the optimization problems of variational algorithms via calculating Hessians on quantum computers efficiently for the landscape of variational classifiers. In practice, there have been a handful of research works exploring the applications of quantum machine learning in drug discovery. In 2021, Batra et al.¹⁶ illustrated the QML applications in drug discovery by comparing the performance of QSVC, with classical and hybrid approaches after compressing SARS-CoV-2 data. It has been demonstrated that quantum computers have the potential to handle "very large" drug discovery data sets with thousands of molecules. Suzuki et al.²⁷ predicted the toxic level of 221 phenols with a hybrid quantum–classical approach and outperformed the classical linear regression algorithm. Later, Liu et al.²¹ incorporated hybrid quantum generative adversarial networks (QGANs) to learn the complex patterns in molecules, quantum convolutional neural networks (QCNNs) for classification of protein packets, and quantum variational autoencoders (QVAE) to generate small molecules. Bhatia and Zheng³⁰ modeled several chemical reactions using theoretical quantum computational models.

Another hybrid quantum algorithm with a restricted Boltzmann machine was used to calculate the electronic ground state energy of molecules.³¹ Sajjan et al.¹⁴ presented a brief review of well-known quantum machine learning algorithms for various physicochemical applications. Recently, Mensa et al.³² investigated the performance of the classical algorithm with quantum kernel estimation for ligand-based virtual screening (LB-VS) on ADRB2 and COVID-19 data sets. Moreover, the performance of the quantum algorithm is tested on an IBM quantum processor and claimed that it can outperform the best classical variants.

III. METHODOLOGY

We designed a quantum machine learning framework for predicting the ADME-Tox properties of chemical compounds in drug discovery. The classical data are used to predict properties with the quantum support vector classifier (QSVC) algorithm and compared its performance against best known classical algorithms.

III.A. ADME-Tox Databases. To explore the diversity and complexity of ADME-Tox properties, we used four chemical compound data sets, i.e., HIA (Human Intestinal Absorption), CYP2D6 Substrate, DILI (Drug Induced Liver Injury), and Carcinogens to predict features accurately given a drug candidate's structural information. All data sets are collected from the Therapeutic Data Commons (TDC),³³ providing several data sets for AI/ML tasks spread across therapeutic modalities (small molecules, macromolecules, cell and gene

therapies) for efficacious medicine development and enhanced patient safety throughout the lifecycle of a medicine.

- The HIA data set consists of information about the absorption of drugs in the human gastrointestinal tract. This data set is commonly used in drug discovery and development to assess the potential of oral absorption. It is an important roadblock in the formulation of new drug candidates. 578 druglike molecules with their SMILES string are used to differentiate the badly absorbed chemical compounds from those that are well absorbed.

- The CYP2D6 substrate data set contains information on 664 drugs and their interaction with the CYP2D6 enzyme, which results in the odemethylation of dextromethorphan in the human liver. It is a crucial enzyme responsible for catalyzing the metabolism of various drugs and xenobiotics in the human body. Given a SMILES string of drugs, the task is to predict whether a drug is a substrate to an enzyme or nonsubstrate.

- The DILI data set consists of the FDA's 475 approved drugs with their potential for causing drug-induced liver injury (DILI) in humans (1) or no-DILI (0) concern. It is a major safety concern in drug development and can lead potentially to impacting drug efficacy and patient safety. It contains information about the chemical structures of various drugs, and hepatotoxicity data associated with liver injury. Given a chemical structure and SMILES string, the objective is to predict whether a drug can cause liver injury or not.

- The Carcinogens (CARC) data set contains information on chemical compounds that can be classified as carcinogenic, i.e., drugs that have the potential to cause cancer. It remains a challenging problem in drug development due to limited available data. The data set of 275 drugs with their SMILES strings is used to identify carcinogenic or noncarcinogenic chemical compounds.

III.B. SVC and QSVC. Support vector classifier (SVC) is a well-known classical machine learning algorithm, also called the "kernel" method, used to perform classification and regression tasks. Suppose N training data points (x_i) and associated labels $y_i \in \{-1, 1\}$ are given, which are spattered in D dimensions, where $1 \leq i \leq N$. The objective is to find a hyperplane that helps us to separate our space into classes by maximum margin. In SVC, it computes the inner product between pairs of data points $\langle x_i | x_j \rangle \in \mathbb{R}$. In the case where the data points cannot be separable linearly, the input data points are transformed to high-dimensional feature space (φ) via a mapping function and a hyperplane determined with a maximum margin. The technique "kernel trick" in SVC enables handling of nonlinear data points, which relies on the inner product between pairs of mapping kernel functions such that $K(x_i, x_j) = \varphi(x_i) \cdot \varphi(x_j)$. Thus, the optimization objective function of SVC with the kernel trick is given as

$$\begin{aligned} \max f(c_1, \dots, c_N) &= \sum_{i=1}^N c_i - \frac{1}{2} \sum_{i=1}^N \sum_{j=1}^N y_i c_i (\varphi(x_i) \cdot \varphi(x_j)) y_j c_j \\ &= \sum_{i=1}^N c_i - \frac{1}{2} \sum_{i=1}^N \sum_{j=1}^N y_i c_i K(x_i, x_j) y_j c_j \end{aligned} \quad (1)$$

subject to $\sum_{i=1}^N c_i y_i = 0$ and $0 \leq c_i \leq 1/2N\lambda$, where λ controls the hard margin classifier. Although, various kernel functions exist such as linear, polynomial, Gaussian (RBF), sigmoid, etc. to solve different problems.

The kernel-based learning methods have been successfully applied in problems dealing with highly dimensional input spaces.

The quantum support vector classifier (QSVC) is an extension of the classical support vector classifier (SVC) that incorporates a quantum feature space for enhanced computational power. The quantum feature space $|\varphi(x_i)\rangle\langle\varphi(x_j)|$ is a high-dimensional complex-valued Hilbert space, which allows for the exploitation of quantum computing capabilities. An architecture of QSVC is shown in Figure 2. Here, a quantum kernel function

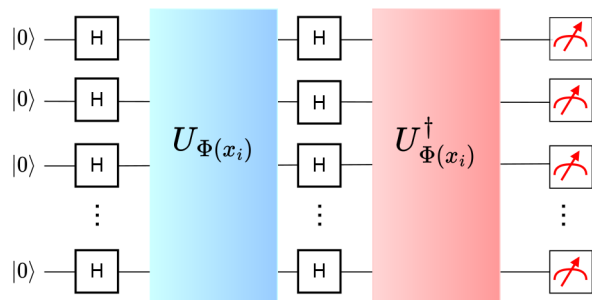


Figure 2. A generalized quantum circuit architecture of the quantum support vector classifier. It consists of the encoding circuit, followed by processing (feature map embedding and inverse of it) and measurement at the end.

is employed to map the data into a quantum feature space represented as

$$K(x_i, x_j) = |\langle\varphi(x_i)|\varphi(x_j)\rangle|^2 \quad (2)$$

where $\varphi(x_i)$ denotes that the first step is to encode classical points $x \in \mathbb{R}^n$ into quantum data using an n -qubit parametrized quantum circuit (PQC) $|\varphi(x)\rangle = U(x)|0^n\rangle$, where U is a unitary operation. We used the ZZFeaturemap with a linear entanglement layer (depth = 2). Although, we can vary the depth of the feature map circuit to introduce more entanglement and repeat ($\times l$) the encoding circuit. The number of qubits depends on the number of features outlined in our data set. The quantum kernel is estimated by evolving a reference state $|0^n\rangle$ as

$$K(x_i, x_j) = |\langle 0^n | U^\dagger(x_i) U(x_j) | 0^n \rangle|^2 \quad (3)$$

The quantum circuit with linear entanglement for eight-dimensional classical input features is given in Figure 3, where H denotes the Hadamard gate to create superposition, and $P(\theta)$ is a phase gate. A unitary operation (U) is applied to quantum registers initialized in the $|0\rangle$ state, and then the inverse operation $U^\dagger(x)$ is applied. Finally, a measurement operator is applied, which estimates the quantity of interest (i.e., the target variable).

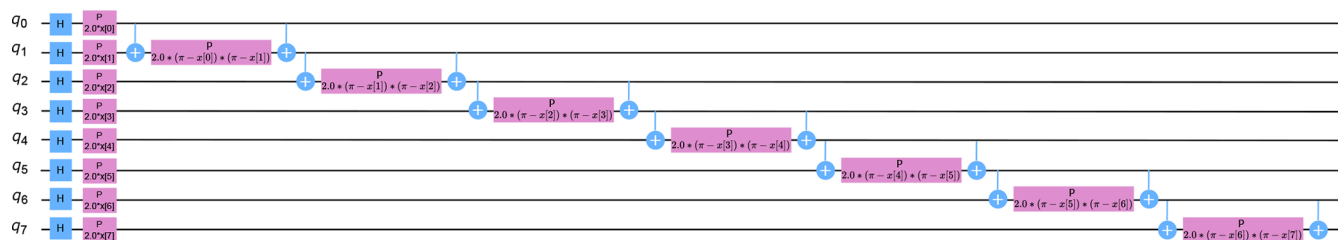


Figure 3. A quantum circuit of eight-dimensional ZZFeaturemap. The qubits are linearly entangled with each other, and the depth is kept as 1. The total number of qubits depends on the number of classical data points.

III.C. Feeding Molecular Descriptors via Quantum Encoding. Our QML framework is associated with the open-source software suite “RDKit” to extract the standard molecular features in SMILES to handle molecular structures in a machine-processable format. It is used to generate RDKit fingerprints of molecules with a default size of 2048 bits and a path length of seven bonds. Due to the limitations of current quantum hardware, it is impractical to process or manipulate classical bit strings of such large sizes directly on quantum computers. To handle this, we used a feature reduction method, “principal component analysis (PCA),” to compress thousands of molecular descriptors, which is the most popular dimension reduction method and widely used in drug discovery. In experiments, we reduced RDKit fingerprints from 2048 features to 2, 4, 8, and 16 to retain most of the information. Due to the low number of qubits available on current gate-based quantum hardware, reducing the dimension of the data is a must. For a fair comparison, we compared the QSVC and classical SVC learning with fewer feature representations.

After generating RDKit fingerprints and reducing the dimension, each classical data feature is normalized and used as angles in the parametrized quantum circuit. Finally, the classical feature vectors are encoded into quantum states via a ZZFeaturemap parametrized circuit, and the quantum kernel is evaluated.

IV. RESULTS AND DISCUSSIONS

Before we move on to the discussion of the experiment, it is also important to provide a brief overview of the parameters our

Table 1. List of Parameters Used in the Experiments

Quantum Support Vector Classifier (QSVC)	
entanglement	linear
depth (rep)	2
embedding scheme	qasm_simulator (qasm) statevector_simulator (SV)
quantum hardware	qasm_noise (p_error= 0.05)
cost (c)	16-qubit IBMQ_Guadalupe default (1.0)
Support Vector Classifier (SVC)	
kernel	linear
cost (c)	default (1.0)
Adaboost Algorithm (ADB)	
n_estimators	50
learning_rate	0.01
Logistic Regression (LR)	
penalty	default = “l2”
solver	lbfgs

Table 2. Classification Performance Metrics of QSVC on Considering 16 Features on the qasm Noise Model

metrics	ADME data set: HIA				ADME data set: CYP2D6			
	fold1	fold2	fold3	fold4	fold1	fold2	fold3	fold4
accuracy	0.863	0.881	0.881	0.863	0.706	0.664	0.746	0.735
precision	0.703	0.750	0.774	0.777	0.842	0.730	0.847	0.752
recall	0.918	0.785	0.889	0.792	0.694	0.657	0.729	0.800
F-score	0.796	0.767	0.827	0.785	0.761	0.691	0.784	0.775
metrics	toxicity data set: DILI				toxicity data set: CARC			
	fold1	fold2	fold3	fold4	fold1	fold2	fold3	fold4
accuracy	0.757	0.841	0.766	0.849	0.821	0.785	0.845	0.747
precision	0.796	0.862	0.775	0.872	0.907	0.895	0.900	0.844
recall	0.741	0.814	0.789	0.842	0.830	0.767	0.849	0.730
F-score	0.727	0.818	0.782	0.817	0.867	0.826	0.873	0.783

model uses to evaluate and simulate the ADME and Tox properties of chemical compounds in drug discovery. In order to compare the aforementioned classification efforts, we computed the performance of the QSVC model by calculating the area under the curve of the receiver operating characteristic (AUC ROC) curve, classification accuracy (ACC), precision, recall, and F-score performance metrics. The receiver operating characteristic (ROC) curve is indeed a widely used evaluation metric in various fields, including the medical, chemistry, and physics field. A higher area under the curve indicates better model performance, which signifies a higher discrimination capacity of the classifier. To verify the effectiveness and robustness of the quantum model fit in this study, we plotted the AUC ROC of QSVC across different quantum simulators and numbers of features of different ADME-Tox data sets.

To showcase the potential advantage of a quantum machine learning algorithm, the proposed framework conducted experiments in two phases: In the initial phase, the experiments were executed in a noiseless quantum environment with the python-based Qiskit's state vector simulator (SV), and qasm simulator (QA), which means that the simulations assumed perfect conditions without any form of noise or errors.³⁴

In the subsequent phase, the simulations were adjusted to introduce noise factors commonly encountered in quantum processors. We apply our method to simulate the quantum circuit by adding depolarizing noise to all single-qubit gates and two-qubit gates using a qasm simulator with noise (QN). These simulations aimed to emulate the conditions of actual IBM processors, giving a more realistic assessment of the QSVC method's performance for all of the mentioned data sets. The depolarizing channel depolarizes a state of qubit into a completely mixed state of $1/2$ with probability p , and the state is left unchanged with $1 - p$ probability.

In this study, we consider that the quantum channel acting on an arbitrary quantum state is the depolarizing channel. It is a widely applied channel model used to represent the decoherence effects that produce errors in quantum information.⁹ The probability of destroying the qubit's state depends on the specific characteristics of the depolarization channel, such as its strength or fidelity. The Kraus representation provides a way to describe the evolution of a quantum system ρ under the influence of noise \mathcal{E} or errors, as

$$\mathcal{E}(\rho) = \sum_k E_k \rho E_k^\dagger \quad (4)$$

where E_k denotes the Kraus operator and satisfies $\sum_k E_k^\dagger E_k = I$.

The depolarizing channel consists of each bit flip, phase flip, and combined flip with the same probability $p/3$. It evolves a density matrix as

$$\rho \rightarrow \mathcal{E}_{\text{DP}}(\rho) = (1 - p)\rho + \frac{p}{3}(X\rho X + Y\rho Y + Z\rho Z) \quad (5)$$

where X , Y , and Z are Pauli gates. We used a custom noise model by adding errors on single-qubit and two-qubit gates with a probability ($p = 0.05$) and tested the quantum model on a qasm simulator. The list of parameters used in the experiments is given in Table 1.

IV.A. Application of QSVC to Predict ADME Properties.

For model development and testing, the synthetic minority oversampling technique (SMOTE) is used to handle the imbalance data set problem by introducing artificial minority instances over three data sets. For representation, the number of chemical compounds of each class is denoted as class:(number of samples before)number of samples after applying SMOTE. In CARC data set, carcinogens are 1:(54)138 and noncarcinogens as 0:(198)197. In the HIA data set, the class absorption was 1:(448)432 and nonabsorption was 0:(72)224, and in the CYP2D6 data set, the substrate was 1(169)344 and the nonsubstrate was 0:(431)430 chemical compounds. To assess the average method performance, each simulation involving both classical machine learning models and quantum classifiers is implemented using 4-fold cross-validation. Table 2 presented the classification metrics of QSVC for predicting ADME-Tox properties using 4-fold cross validation with the qasm noise model. Figure 4a–d present the true positive rate versus false positive rate considering different numbers of features (2, 4, 8, and 16) and different quantum simulators for all ADME-Tox data sets.

Property Analysis of Human Intestinal Absorption (HIA).

We initially demonstrated the application of a quantum classifier to classify the absorption and nonabsorption molecules in the HIA data set. We tested the QSVC on noiseless quantum simulators and a noise based simulator, considering different numbers of features after applying PCA. We observed that with the increase in the number of features, the performance of QSVC gets improved in terms of AUC ROC, as shown in Figure 5c. Thus, QSVC performed better than classical counterparts in predicting ADME-Tox properties after reducing the number of features (2, 4, 8, and 16), which can be implemented on the current available quantum infrastructure. Although, the classical SVC achieved a better AUC ROC on considering whole 2048 bit RdKit fingerprints.

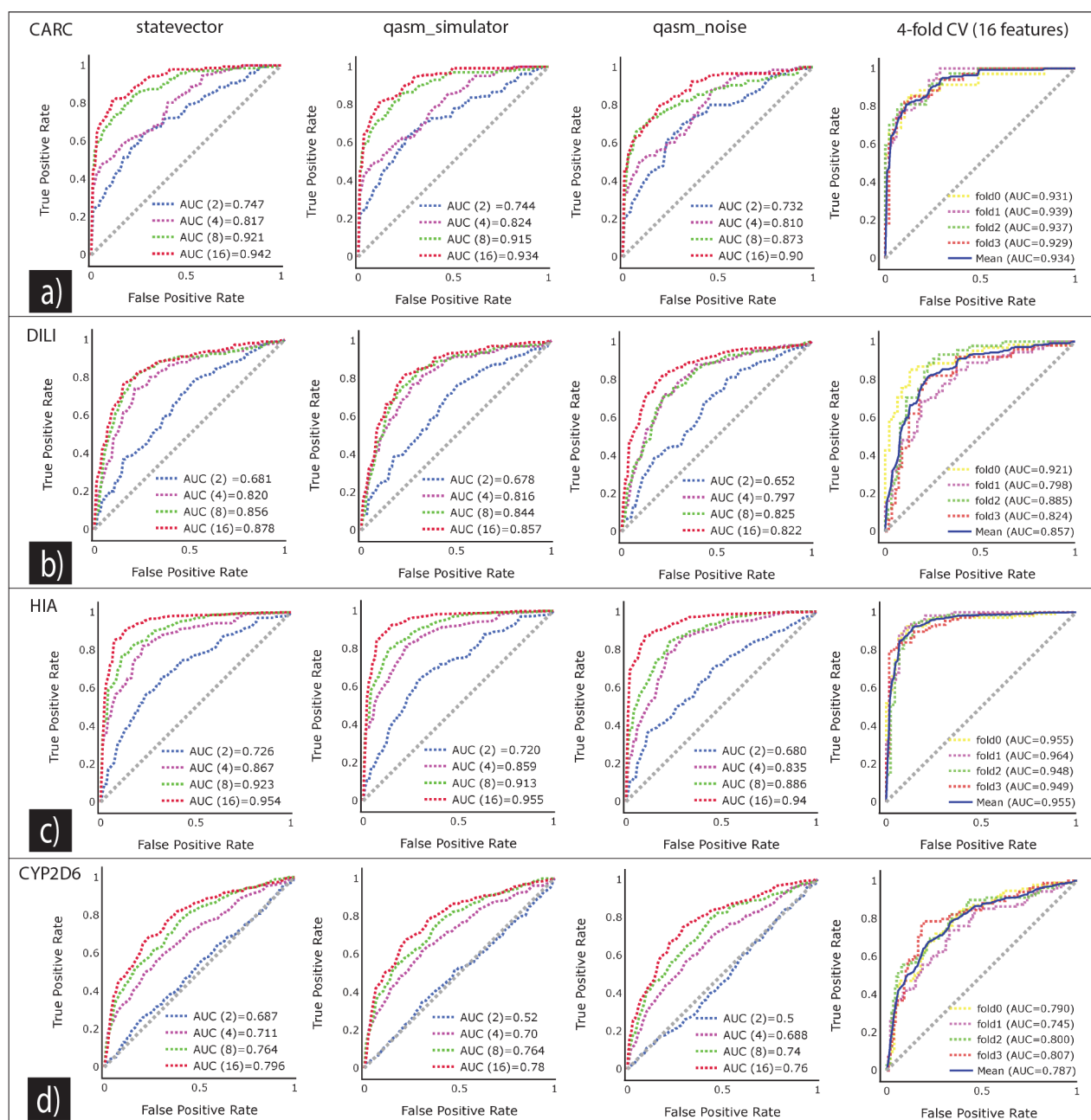


Figure 4. True positive rate vs false positive rate plotted considering different numbers of features and different quantum simulators. (a–d) Simulation results using 4-fold cross-validation across all data sets (CARC, DILI, HIA, and CYP2D6), respectively. The QSVC shows promising results for CARC and HIA data sets with mean (AUC ROC > 0.90) and around 0.85 for the DILI data set. (d) AUC remains below 80% for the CYP2D6 data set on considering 16 features.

According to the simulation results, the QSVC model showed promising results across all of the simulators AUC (SV = 0.954, QA = 0.955, and QN = 0.94) with 16 features. We noticed that the mean AUC ROC of the quantum model with the noise model is also in line with noiseless simulators. Although, the performance of QSVC depends upon the number of features selected from the molecular data set. The F-score (0.20) remains lower with two input features, as shown in Figure 6c. Later, it tends to perform substantially better with more features and achieved an F-score (0.86) irrespective of the quantum simulator.

Property Analysis of CYP2D6 Substrates. Particularly, the quantum classifier achieved an AUC ROC less than 0.80 even

with 16 features among all of the simulators (i.e., 0.77–0.79), as shown in Figure 5d. The range of mean AUC ROC remains between 0.48 and 0.79 by varying the number of features (2–16). Its performance is significantly less compared to all considered ADME-Tox data sets. Moreover, the F-score lies in the range of 0.68–0.82 across all quantum simulators, as depicted in Figure 6d. It has been noticed that classical SVC performed better than quantum variants considering 2048 bit RDKit fingerprints and achieved an AUC ROC around 0.856.

IV.B. Application of QSVC to Predict Toxicity. *Property Analysis of Drug-Induced Liver Injury (DILI).* In our study, the DILI data set consists of 475 drugs, and we selected molecules of bond length 7 causing liver injury (209) and no-DILI (218)

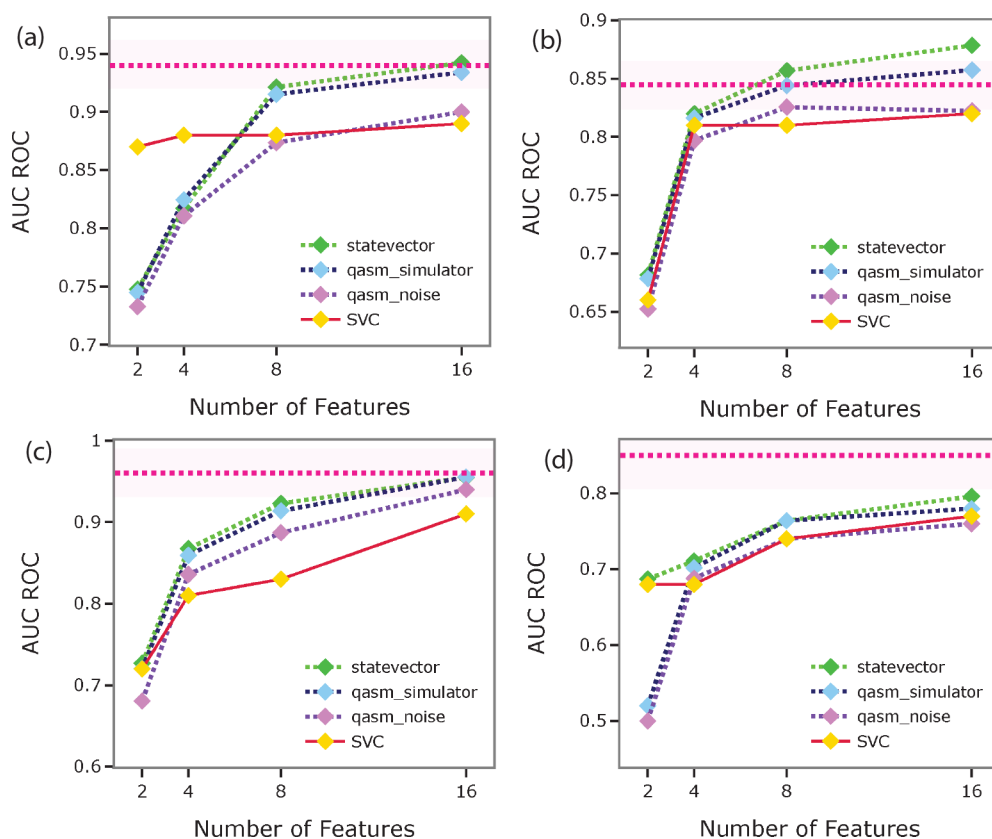


Figure 5. The mean AUC ROC curves of the quantum classifier across all quantum simulators. Here, we report the mean AUC ROC results with different numbers of features used to train the QSVC model. (a–d) CARC, DILI, HIA, and CYP2D6 data sets with the PCA feature reduction method. The state vector backend is a green dotted line, the (qasm simulator (QA) is in blue, and the qasm simulation with noise (QN) is represented with a purple dotted line. The classical SVC is denoted by a solid line (red), and the shaded line is for SVC considering 2048 bit RDKit fingerprints.

concern. We observed that the quantum model is able to correctly classify the molecules causing liver injury versus no injury concern with 168 molecules of each class out of their respective proportion in the data set. The QSVC model performed slightly better at predicting active DILI-Concern compounds with an AUC ROC around 0.87 with 16 features, as shown in Figure 5b. The F-score remains around 0.50 with two data points. It has been noticed that the performance of the quantum model remains constant with increasing the number of features (4, 8 and 16); i.e., F-score lies in 0.7–0.8, as shown in Figure 6b. The mean AUC ROC of classical SVC remains in between 0.65 and 0.82 on varying the number of features.

Property Analysis of Carcinogens (CARC). Here, we have applied the SMOTE technique to balance the class distribution in the CARC data set. Now, it consists of a total of 335 drugs in which the carcinogens (active) equal 138 and the non-carcinogens (inactive) equal 197. The QSVC shows good performance in differentiating the active (110) versus inactive molecules (190). The quantum model provides a mean AUC ROC (0.75) with only two features and achieved the highest AUC ROC (SV = 0.942, QA = 0.934, and QN = 0.90) with 16 input features, as shown in Figure 5a. The quantum classifier achieved an F-score around 0.88. Although, its performance with the qasm noise model remains lower as compared to the noiseless quantum simulators with 16 features. The mean AUC ROC of classical SVC remains in between 0.68 and 0.90 on varying the number of features. Although, it performed better than quantum variants considering whole 2048 bit RDKit fingerprints, achieving an AUC ROC around 0.996.

IV.C. Comparison with Classical Counterparts. In this section, we evaluated whether the quantum classifier can do well on available quantum hardware. Here, we performed the experiments of ADMe-Tox data sets (8 and 16 input features) on a 16 qubit IBM quantum Guadalupe. Moreover, the performance of the quantum support vector classifier (QSVC) is compared with its classical variant SVC, adaboost classifier, logistic regression, and k-nearest neighbors (KNN) algorithm. The classical KNN is widely used and makes predictions on the basis of the average or majority vote of k nearest data points in the feature space. We performed experiments of SVC with RDKit and Morgan fingerprint bit strings. Although, we computed the results of classical counterparts considering only RDKit fingerprints. The maximum bond lengths are set as 2 and 7 for Morgan and RDKit fingerprints, respectively. For a fair comparison between classical and quantum, we reported the mean result across 4-fold cross-validation for all simulations.

To ensure the validity of our model's interpretability, we conducted a verification process using diverse data sets (CARC, DILI, HIA, and CYP2D6) that shared an identical number of input features. This rigorous examination allowed us to confirm the consistency and reliability of our model's interpretive capabilities across various data sets. The improved performance of the QSVC algorithm can be attributed to a larger quantum feature space and an enhanced expressiveness of the quantum feature map, enabling appropriate separation between badly absorbed/well absorbed, DILI/no-DILI, and many more. A noteworthy observation when comparing classical and quantum methodologies is that the performance of QSVC either remains

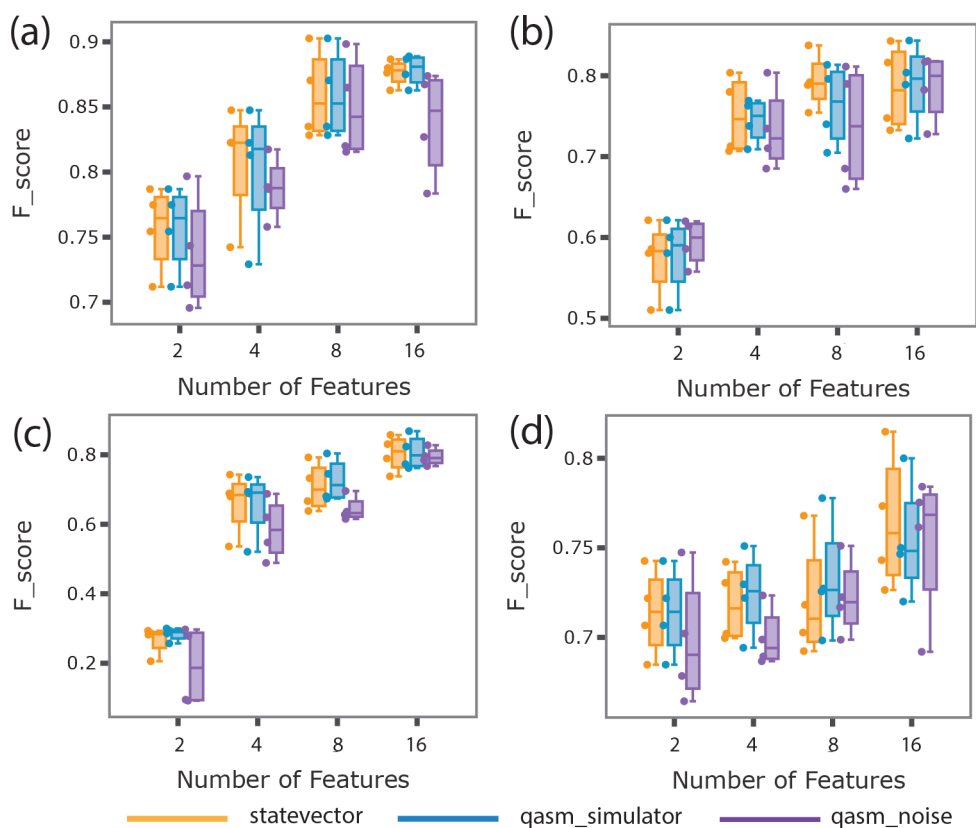


Figure 6. Graphical representation of boxplots for the F-score performance metric of quantum simulators (state vector as orange, qasm simulator in blue, and qasm with noise as purple). Here, we applied four-fold cross validation in all simulations and presented the F-scores of all data sets (CARC, DILI, HIA, and CYP2D6) with different numbers of features among all quantum simulators in a–d, respectively. In boxplots, the median value is denoted by the horizontal line, and the box defines upper and lower quartiles. The data points are the statistical outliers.

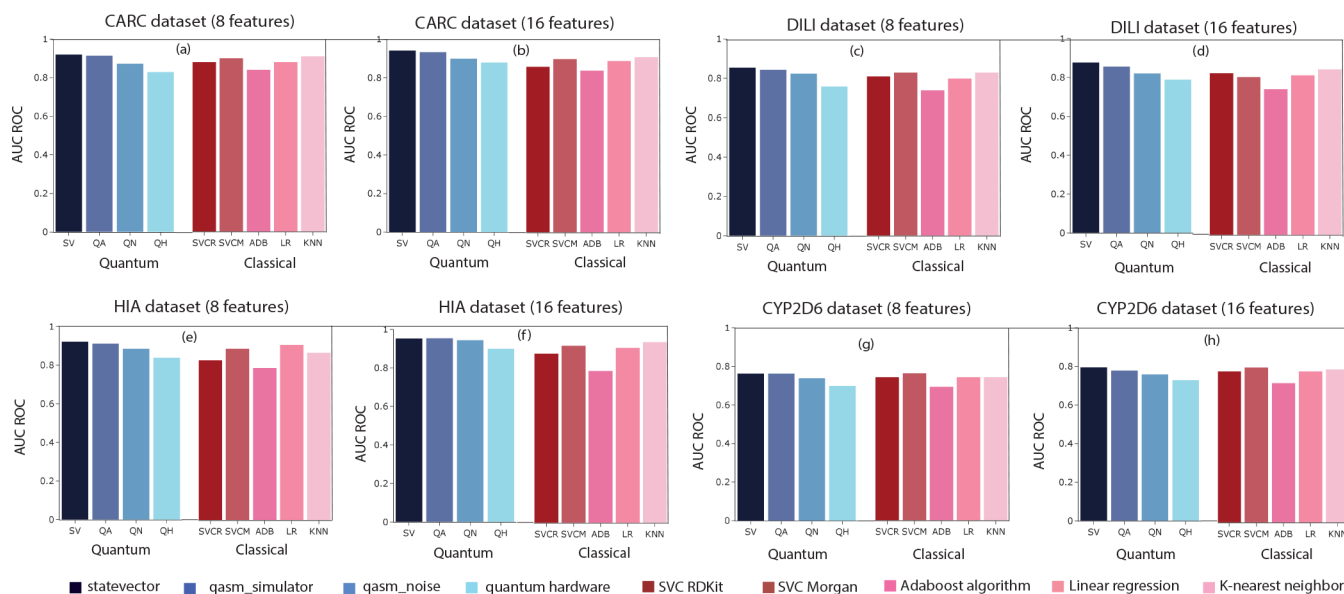


Figure 7. Performance of QSVC vs classical algorithms. The performance of QSVC is tested on noiseless and noisy simulators and quantum hardware (16 qubits IBMQ Guadalupe). Moreover, we tested the classical algorithms (SVCR, ADB, LR, and KNN) with RDKit and classical SVMC with Morgan fingerprints on considering fewer feature representations. We reported the mean result of AUC ROC across 4-fold cross-validation for all simulations.

consistent or improves as the number of features increases. This trend suggests the possibility of a quantum advantage within QSVC, indicating its potential for enhanced performance compared to classical approaches.

In the case of CARC and HIA data sets, we found that the AUC ROC of QSVC on quantum hardware remains equivalent to SVC and marginally lower than the KNN algorithm, with eight data points, as shown in Figure 7b,f. We observed that on

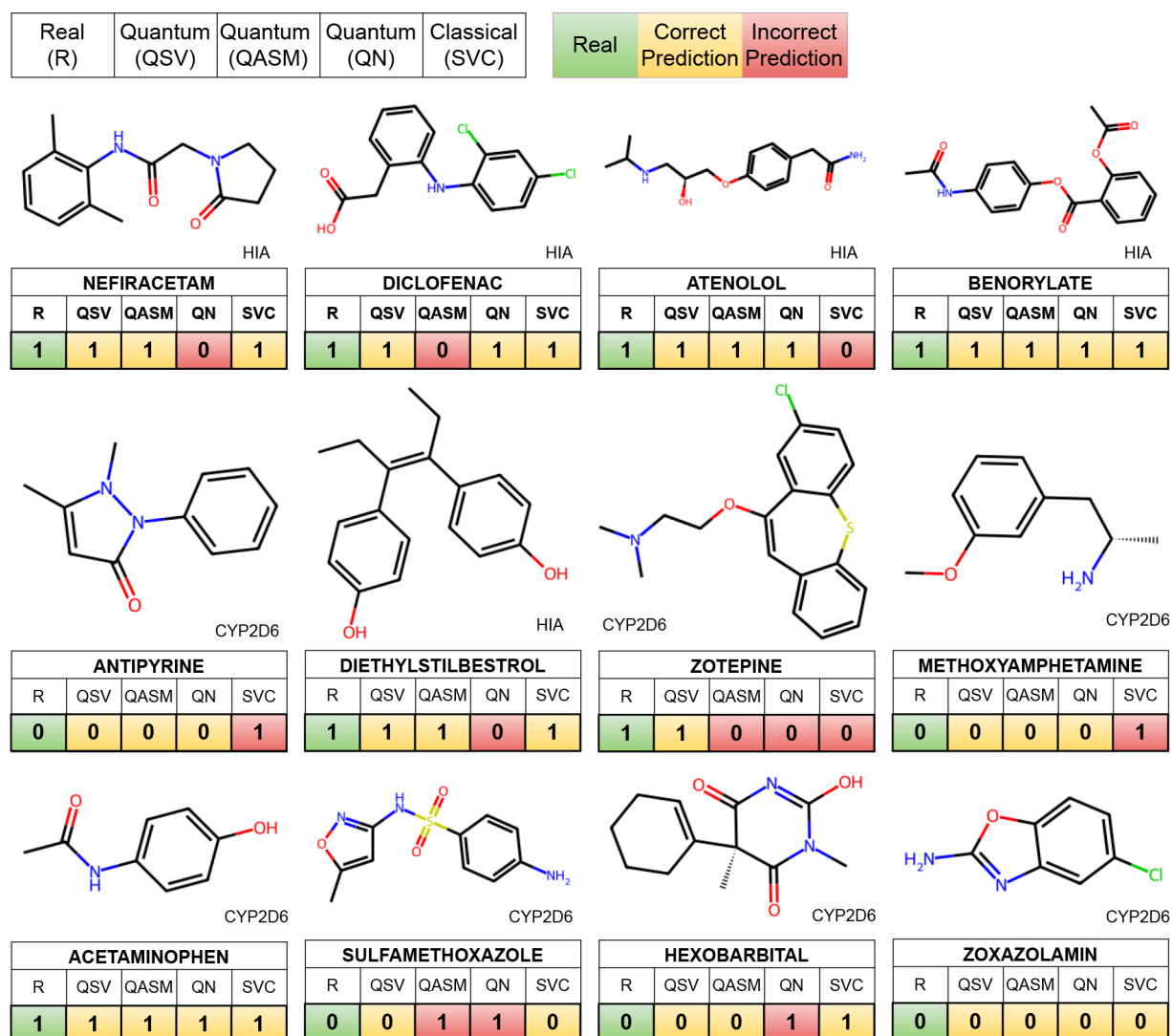


Figure 8. Prediction of molecules by QSVC and SVC. Molecules are randomly selected from HIA and CYP2D6 data sets. The prediction is made by quantum simulators and classical SVC against real labels.

considering the number of features (>8), the quantum algorithm outperformed its classical variant, as shown in Figure 7a,e. Although, the classical KNN algorithm provides marginally better classification results with Morgan fingerprints (i.e., better mean AUC ROC values). For the DILI data set, SVC performed better than QSVC with Morgan fingerprints and eight data points, as shown in Figure 7d. For the CYP2D6 data set, the mean AUC ROC of QSVC remains below 0.80 and marginally better than its variant. But, KNN with Morgan fingerprints shows promising results considering 16 features of the CYP2D6 data set, as shown in Figure 7g,h. It has been noticed that the performance of QSVC remains less affected with the increase in number of features and in the presence of qasm simulator noise. The QSVC algorithm on quantum hardware produces promising results that are in line with the qasm simulator and state vector results. In Figure 8, randomly selected molecules from the HIA and CYP2D6 data sets are utilized to demonstrate the molecule prediction capabilities of both quantum QSVC and classical SVC.

Therefore, the quantum kernel has captured the complicated relationships among the molecular features and leveraged the increased dimensionality effectively compared to its classical

variant. It is worth noting that the performance of quantum kernels can be influenced by various factors, such as the specific quantum computing algorithm or approach used, the nature (i.e., characteristics, dimensionality, noise) of the data set, and the real quantum hardware employed.

V. CONCLUSIONS

In this Article, we designed a quantum machine learning framework to identify the ADME-Tox properties of chemical compounds in drug discovery. Due to currently available quantum computers with limited qubit counts, we reduced the dimensionality of data sets to accommodate the capabilities of available quantum hardware. We demonstrated the performance of a quantum support vector classifier using IBM quantum simulators and systems. A quantum algorithm can provide a significant advantage over classical counterparts in certain instances, depending upon the number of features selected. We investigated whether an analysis of molecular data can benefit from the use of quantum computers after reducing the problem to a certain level, which can be affordable. Currently, there are no apparent reasons to doubt that the quantum benefit observed in proof-of-principle applications would diminish when simulating


a larger number of features with 40–60 qubits. However, it is important to note that achieving a quantum advantage in drug discovery requires advancements in quantum hardware, software, and algorithm development. It should be noted that classical SVC achieved a better mean AUC ROC overall on considering 2048 RDKit fingerprints. We observed that the quantum kernel method is well-suited for predicting ADME-Tox properties by achieving an F-score (0.80–0.90) and AUC ROC (0.85–0.95) with only 16 features, except the DILI data set. Moreover, the quantum classifier has correctly predicted the targets with simulated backends even in the presence of noise and enabling more comprehensive analysis of drug candidates. We can conclude that the quantum algorithms have the potential to enable more complex molecular simulations and calculations, allowing for more accurate predictions of ADME-Tox properties.

AUTHOR INFORMATION

Corresponding Authors

Amandeep Singh Bhatia – School of Electrical and Computer Engineering, Purdue University, West Lafayette, Indiana 47907, United States; Email: bhatia87@purdue.edu

Mandeep Kaur Saggi – Department of Chemistry, Purdue University, West Lafayette, Indiana 47907, United States; Email: msaggi@purdue.edu

Sabre Kais – Department of Chemistry, Purdue University, West Lafayette, Indiana 47907, United States;  orcid.org/0000-0003-0574-5346; Email: kais@purdue.edu

Complete contact information is available at:
<https://pubs.acs.org/10.1021/acs.jcim.3c01079>

Author Contributions

A.S.B. and M.K.S. conceived the basic idea and designed the framework. A.S.B. and M.K.S. performed the experiments under the guidance of S.K. A.S.B. and M.K.S. wrote the manuscript. All authors contributed to conceptualization and revising the manuscript.

Notes

The authors declare no competing financial interest.

ACKNOWLEDGMENTS

We would like to thank the Elmore Family School of Electrical and Computer Engineering (ECE) Emerging Frontiers Center at Purdue University for the financial support. S.K. also acknowledges funding from the National Science Foundation under award no. 1955907.

REFERENCES

- (1) Krejsa, C.; Horvath, D.; Rogalski, S.; Penzotti, J.; Mao, B.; Barbosa, F.; Migeon, J. Predicting ADME properties and side effects: the BioPrint approach. *Curr. Opin. Drug Discovery Dev.* **2003**, *6*, 470–480.
- (2) Selick, H.; Beresford, A.; Tarbit, M. The emerging importance of predictive ADME simulation in drug discovery. *Drug Discovery Today* **2002**, *7*, 109–116.
- (3) Waring, M. J.; Arrowsmith, J.; Leach, A. R.; Leeson, P. D.; Mandrell, S.; Owen, R. M.; Pairedeau, G.; Pennie, W. D.; Pickett, S. D.; Wang, J.; Wallace, O.; Weir, A. An analysis of the attrition of drug candidates from four major pharmaceutical companies. *Nat. Rev. Drug Discovery* **2015**, *14*, 475–486.
- (4) Wang, Y.; Xing, J.; Xu, Y.; Zhou, N.; Peng, J.; Xiong, Z.; Liu, X.; Luo, X.; Luo, C.; Chen, K.; Zheng, M.; Jiang, H. In silico ADME/T modelling for rational drug design. *Quant. Rev. Biophys.* **2015**, *48*, 488–515.

(5) Muster, W.; Breidenbach, A.; Fischer, H.; Kirchner, S.; Müller, L.; Pähler, A. Computational toxicology in drug development. *Drug Discovery Today* **2008**, *13*, 303–310.

(6) Maltarollo, V.; Gertrudes, J.; Oliveira, P.; Honorio, K. Applying machine learning techniques for ADME-Tox prediction: a review. *Expert Opin. Drug Metab. Toxicol.* **2015**, *11*, 259–271.

(7) Korotcov, A.; Tkachenko, V.; Russo, D.; Ekins, S. Comparison of deep learning with multiple machine learning methods and metrics using diverse drug discovery data sets. *Mol. Pharmaceutics* **2017**, *14*, 4462–4475.

(8) Ekins, S.; Puhl, A.; Zorn, K.; Lane, T.; Russo, D.; Klein, J.; Hickey, A.; Clark, A. Exploiting machine learning for end-to-end drug discovery and development. *Nat. Mater.* **2019**, *18*, 435–441.

(9) Nielsen, M.; Chuang, I. *Quantum Computation and Quantum Information*; American Association of Physics Teachers, 2002.

(10) Cao, Y.; Romero, J.; Aspuru-Guzik, A. Potential of quantum computing for drug discovery. *IBM J. Res. Dev.* **2018**, *62*, 6:1.

(11) Carleo, G.; Cirac, I.; Cranmer, K.; Daudet, L.; Schuld, M.; Tishby, N.; Vogt-Maranto, L.; Zdeborová, L. Machine learning and the physical sciences. *Rev. Mod. Phys.* **2019**, *91*, 045002.

(12) von Lilienfeld, O. A.; Muller, K.-R.; Tkatchenko, A. Exploring chemical compound space with quantum-based machine learning. *Nat. Rev. Chem.* **2020**, *4*, 347–358.

(13) Orús, R.; Mugel, S.; Lizaso, E. Quantum computing for finance: Overview and prospects. *Reviews In Physics* **2019**, *4*, 100028.

(14) Sajjan, M.; Li, J.; Selvarajan, R.; Sureshbabu, S.; Kale, S.; Gupta, R.; Singh, V.; Kais, S. Quantum machine learning for chemistry and physics. *Chem. Soc. Rev.* **2022**, *51*, 6475.

(15) Von Lilienfeld, O. Quantum machine learning in chemical compound space. *Angew. Chem., Int. Ed.* **2018**, *57*, 4164–4169.

(16) Batra, K.; Zorn, K.; Foil, D.; Minerali, E.; Gawriljuk, V.; Lane, T.; Ekins, S. Quantum machine learning algorithms for drug discovery applications. *J. Chem. Inf. Model.* **2021**, *61*, 2641–2647.

(17) Li, J.; Alam, M.; Congzhou, M.; Wang, J.; Dokholyan, N.; Ghosh, S. Drug discovery approaches using quantum machine learning. *2021 58th ACM/IEEE Design Automation Conference (DAC)*; IEEE, 2021; pp 1356–1359.

(18) Kao, P.-Y.; Yang, Y.-C.; Chiang, W.-Y.; Hsiao, J.-Y.; Cao, Y.; Aliper, A.; Ren, F.; Aspuru-Guzik, A.; Zhavoronkov, A.; Hsieh, M.-H.; Lin, Y.-C. Exploring the Advantages of Quantum Generative Adversarial Networks in Generative Chemistry. *J. Chem. Inf. Model.* **2023**, *63*, 3307.

(19) Mustafa, H.; Morapakula, S.; Jain, P.; Ganguly, S. Variational Quantum Algorithms for Chemical Simulation and Drug Discovery. *arXiv* **2022**, arXiv:2211.07854.

(20) Sajjan, M.; Li, J.; Selvarajan, R.; Sureshbabu, S.; Kale, S.; Gupta, R.; Kais, S. Quantum computing enhanced machine learning for physico-chemical applications. *arXiv* **2021**, arXiv:2111.00851.

(21) Liu, Y.; Arunachalam, S.; Temme, K. A rigorous and robust quantum speed-up in supervised machine learning. *Nat. Phys.* **2021**, *17*, 1013–1017.

(22) Bhatia, A.; Saggi, M.; Kumar, A.; Jain, S. Matrix product state-based quantum classifier. *Neural Computation* **2019**, *31*, 1499–1517.

(23) Bhatia, A.; Kais, S.; Alam, M. Handling Privacy-sensitive Clinical Data with Federated Quantum Machine Learning. *Bull. Am. Phys. Soc.* **2023**, Not Yet Published.

(24) Hou, T.; Wang, J.; Zhang, W.; Xu, X. ADME evaluation in drug discovery. 7. Prediction of oral absorption by correlation and classification. *J. Chem. Inf. Model.* **2007**, *47*, 208–218.

(25) Carbon-Mangels, M.; Hutter, M. Selecting relevant descriptors for classification by bayesian estimates: a comparison with decision trees and support vector machines approaches for disparate data sets. *Mol. Inf.* **2011**, *30*, 885–895.

(26) Xu, Y.; Dai, Z.; Chen, F.; Gao, S.; Pei, J.; Lai, L. Deep learning for drug-induced liver injury. *J. Chem. Inf. Model.* **2015**, *55*, 2085–2093.

(27) Suzuki, T.; Katouda, M. Predicting toxicity by quantum machine learning. *J. Phys. Commun.* **2020**, *4*, 125012.

(28) Sen, P.; Bhatia, A.; Bhangu, K.; Elbeltagi, A. Variational quantum classifiers through the lens of the Hessian. *PLoS One* **2022**, *17*, No. e0262346.

(29) Cerezo, M.; Arrasmith, A.; Babbush, R.; Benjamin, S. C.; Endo, S.; Fujii, K.; McClean, J. R.; Mitarai, K.; Yuan, X.; Cincio, L.; Coles, P. J. Variational quantum algorithms. *Nat. Rev. Phys.* **2021**, *3*, 625–644.

(30) Bhatia, A.; Zheng, S. A quantum finite automata approach to modeling the chemical reactions. *Frontiers In Physics* **2020**, *8*, 547370.

(31) Xia, R.; Kais, S. Quantum machine learning for electronic structure calculations. *Nat. Commun.* **2018**, *9*, 4195.

(32) Mensa, S.; Sahin, E.; Tacchino, F.; Kl Barkoutsos, P.; Tavernelli, I. Quantum machine learning framework for virtual screening in drug discovery: a prospective quantum advantage. *Machine Learning: Science And Technology* **2023**, *4*, 015023.

(33) Huang, K.; Fu, T.; Gao, W.; Zhao, Y.; Roohani, Y.; Leskovec, J.; Coley, C.; Xiao, C.; Sun, J.; Zitnik, M. Therapeutics data commons: Machine learning datasets and tasks for drug discovery and development. *arXiv* **2021**, arXiv:2102.09548.

(34) Anis, M.; Abraham, H.; AduOffei, R.; Agliardi, G.; Aharoni, M.; Akhalwaya, I.; Aleksandrowicz, G.; Alexander, T.; Amy, M.; Anagolum, S. *Qiskit: An Open-Source Framework for Quantum Computing*; Zenodo, **2021**, DOI: [10.5281/zenodo.2562111](https://doi.org/10.5281/zenodo.2562111).